

To appear in the Astrophysical Journal

THE BEAMING PATTERN OF DOPPLER BOOSTED THERMAL ANNIHILATION RADIATION: APPLICATION TO MEV BLAZARS

Jeffrey G. Skibo and Charles D. Dermer

E. O. Hulburt Center for Space Research, Code 7653, Naval Research Laboratory,
Washington, DC 20375-5352

and

Reinhard Schlickeiser

Max-Planck-Institut für Radioastronomie, Postfach 20 24, 53010 Bonn, Germany

ABSTRACT

The beaming pattern of thermal annihilation radiation is broader than the beaming pattern produced by isotropic nonthermal electrons and positrons in the jets of radio-emitting active galactic nuclei which Compton scatter photons from an external isotropic radiation field. Thus blueshifted thermal annihilation radiation can provide the dominant contribution to the high-energy radiation spectrum at observing angles $\theta \gtrsim 1/\Gamma$, where Γ is the bulk Lorentz factor of the outflowing plasma. This effect may account for the spectral features of MeV blazars discovered with the Compton Telescope on the *Compton Gamma Ray Observatory*. Coordinated gamma-ray observations of annihilation line radiation to infer Doppler factors and VLBI radio observations to measure transverse angular speeds of outflowing plasma blobs can be used to determine the Hubble constant.

Subject headings: active galactic nuclei — cosmology: distance scale — galaxies: radio — gamma rays: galaxies — gamma rays: theory

1. Introduction

Observations made with the Compton Telescope (Comptel) on the *Compton Gamma-Ray Observatory* (*CGRO*) reveal the existence of a class of gamma-ray blazars displaying spectral energy distributions peaking in a rather narrow energy band centered at a few MeV (Bloemen et al. 1995; Blom et al. 1995). By combining data from 19 September - 3 October 1991 and 27 December 1991 - 10 January 1992, Bloemen et al. (1995) discovered the first “MeV blazar” GRO J0516-609, which shows a $3-4\sigma$ peak in its νF_ν spectrum in the 1 - 10 MeV energy interval. Only upper limits are measured with Comptel in the 0.75-1 MeV and 10-30 MeV range, although contemporaneous observations with the Energetic Gamma Ray Experiment Telescope (EGRET) on *CGRO* indicate the presence of a weak 3σ excess at photon energies $E > 100$ MeV. The flat spectrum quasars PKS 0506-612 and PKS 0522-611 are both within the 95% Comptel contours of GRO J0516-609, but the former source is the preferred identification due to the more precise EGRET localization, which places only PKS 0506-612 within its 95% confidence contour. This source is reported at the 3.9σ significance level in the Second EGRET catalog (Thomson et al. 1995), but is too weak to be listed as a catalogued EGRET source.

The blazar PKS 0208-512 was detected in analysis of Comptel data by Blom et al. (1995). The strongest signal from PKS 0208-512 was obtained by combining data from 8-13 May 1993 and 3-14 June 1993, yielding a flux in the 1-3 MeV band of $4.1(\pm 0.7) \times 10^{-4}$ photon $\text{cm}^{-2} \text{s}^{-1}$ and upper limits at lower and higher energies in the Comptel energy range. Contemporary observations with EGRET yield a strong > 100 MeV detection of the source 2EG J0210-5051, with PKS 0208-512 located within the 95% confidence contour of this source. The peak in the νF_ν spectrum of PKS 0208-512 occurs at MeV energies, supporting its classification as an MeV blazar. Williams et al. (1995) also report the detection of the gamma-ray source GRO J1753+57 with a spectrum similar to that of the other two MeV blazars. Lack of association of this object with a flat radio spectrum quasar makes this object’s classification uncertain, but one should keep in mind that blazars are highly variable at all wavelengths, so that contemporaneous multiwavelength campaigns could be necessary for proper source identification.

The peaked emission from MeV blazars has been interpreted as Doppler boosted e^+e^- annihilation radiation produced in collimated jets of plasma ejected from a supermassive black hole (Roland & Hermsen 1995; Henri, Pelletier, & Roland 1993). The possible importance of e^+e^- processes and γ - γ opacity effects has been considered by Blandford & Levinson (1994), Böttcher, Mause, & Schlickeiser (1997), and Marcowith, Henri, & Pelletier (1995). No attempt has been made, however, to account for the significant spectral differences between MeV blazars and the > 50 γ -ray blazars detected by EGRET (e.g., von

Montigny et al. 1995), which show strong high-energy radiation extending to GeV and, in a few cases (e.g., Macomb et al. 1996; Schubnell et al. 1996), TeV energies.

In this paper we show that the beaming pattern of thermal Doppler-boosted e^+e^- annihilation radiation is much broader than the beaming pattern produced by nonthermal jet electrons which Compton scatter photons produced outside the jet, whose beaming pattern was recently derived (Dermer 1995; Dermer, Sturmer, & Schlickeiser 1997). We call this latter process external Compton scattering (ECS) and distinguish it from synchrotron self-Compton (SSC) scattering, which has also been proposed as the radiation process yielding blazar gamma radiation (see Marscher & Travis 1996 and references therein). If the high-energy emission in blazars is primarily produced by ECS and, moreover, the annihilation luminosity from thermal e^+e^- pairs is significant, then a class of objects with properties similar to the MeV blazars is a natural consequence of orientation effects when viewing at moderate angles with respect to the axis of the outflowing jet. In addition, we show in Appendix A that if the peaks of MeV blazars are indeed due to Doppler-boosted thermal annihilation radiation, then gamma-ray observations to measure Doppler factors \mathcal{D} coordinated with VLBI radio observations to measure transverse angular speeds μ of outflowing radio blobs in two or more episodes is sufficient to determine the Hubble constant H_0 .

2. Spectra and Angular Distribution of Jet and Accretion-Disk Radiation

We calculate the received spectral flux and radiation pattern from a system consisting of an accretion disk and a relativistic collimated outflow of thermal and nonthermal e^+e^- pairs. We do not attempt to derive the particle distributions self-consistently from first principles. Evolution of nonthermal particles due to radiative losses in outflowing plasma blobs has been treated in detail by Dermer & Schlickeiser (1993) and Dermer et al. (1997), and the formation of a thermalized pair plasma in jets has been considered by Böttcher & Schlickeiser (1996). The emphasis here is rather on the angle-dependence of the received fluxes from the following three spectral components: (1) annihilation radiation from hot thermal pairs in the relativistic outflow; (2) inverse Compton emission from nonthermal pairs in the outflow; and (3) a quasi-isotropic thermal Comptonization spectrum from hot optically thin accretion plasma located near the central supermassive black hole. The central assumption in calculating the jet spectra, as discussed by Dermer & Schlickeiser (1993), is that the particle distribution function is isotropic in the comoving blob frame.

We derive the received spectrum of thermal annihilation radiation. The observed flux density $S(\epsilon; \mu, \phi)$ (erg cm⁻² s⁻¹ ϵ^{-1}) from a blob moving with bulk velocity βc is related

to the emissivity in the comoving frame $j^*(\epsilon^*, \mu^*, \phi^*)$ ($\text{erg cm}^{-3} \text{ s}^{-1} \epsilon^{-1} \text{ sr}^{-1}$) through the relation

$$S(\epsilon; \mu, \phi) = \frac{\mathcal{D}^3(1+z)V^*}{d_L^2} j^* \left[\frac{\epsilon(1+z)}{\mathcal{D}}, \frac{\mu - \beta}{1 - \beta\mu}, \phi \right] \quad (1)$$

(e.g. Begelman, Blandford, & Rees 1984), where $\epsilon = h\nu/m_e c^2$ is the dimensionless photon energy in the stationary frame and V^* is the volume of the blob in the comoving frame. (Hereafter starred quantities refer to the comoving frame, unstarred quantities to the stationary frame.) The direction from the source to the observer is (μ, ϕ) , with μ representing the cosine of the angle between the jet axis and the line of sight, and ϕ representing the azimuthal angle. The Doppler factor $\mathcal{D} \equiv [\Gamma(1 - \beta\mu)]^{-1}$, where the bulk Lorentz factor $\Gamma = (1 - \beta^2)^{-1/2}$, the speed of the blob is βc , and the luminosity distance $d_L = 2c[1 + z - (1 + z)^{1/2}]/H_0$ for a $8\pi G\rho/3H_0^2 = 1$, $\Lambda = 0$ cosmology (Weinberg 1972). The Hubble constant $H_0 = 50h \text{ km s}^{-1} \text{ Mpc}^{-1}$.

We assume that there is a population of thermal pairs with dimensionless temperature $\Theta_a \equiv kT/m_e c^2$ in the outflow. The annihilation emissivity is isotropic in the comoving frame and is given by the expression

$$j_a^*(\epsilon^*, \mu^*, \phi^*; \Theta_a) = \frac{L_a^* \epsilon^*}{4\pi V^*} \exp \left\{ -\frac{1}{\Theta_a} \left[\epsilon^* + \left(\frac{1}{2\epsilon^*} \right) \right] \right\} \cdot \frac{\int_1^\infty d\gamma_r (\gamma_r - 1) \exp[-\gamma_r/(2\Theta_a \epsilon^*)] \sigma_a(\gamma_r)}{\int_1^\infty d\gamma_r (\gamma_r^2 - 1) K_2 \left[\frac{1}{\Theta_a} \sqrt{2(\gamma_r + 1)} \right] \sigma_a(\gamma_r)}. \quad (2)$$

(Svensson 1983; Dermer 1984), where L_a^* is the luminosity of annihilation photons in the comoving frame and K_2 is the modified Bessel function of the second kind. The integration variable $\gamma_r = \mathcal{U}_+ \cdot \mathcal{U}_-$ is the invariant relative Lorentz factor formed from the e^+ and e^- four velocities. The cross section for annihilation, expressed in terms of γ_r , is given by

$$\sigma_a(\gamma_r) = \frac{\pi r_e^2}{\gamma_r + 1} \left\{ \left(\frac{\gamma_r^2 + 4\gamma_r + 1}{\gamma_r^2 - 1} \right) \ln[\gamma_r + (\gamma_r^2 - 1)^{1/2}] - \frac{\gamma_r + 3}{(\gamma_r^2 - 1)^{1/2}} \right\} \quad (3)$$

(e.g. Jauch & Rohrlich 1976), where $r_e = e^2/m_e c^2 = 2.82 \times 10^{-13} \text{ cm}$ is the classical radius of the electron.

Combining equations (1), (2), and (3) we obtain the annihilation flux density $S_a(\epsilon; \mu, \phi)$. The beaming pattern for thermal annihilation radiation is not obvious from the resulting formula. To derive the beaming pattern we approximate the annihilation

emissivity as a delta function centered at unity, which is a reasonable approximation when $\Theta_a \ll 1$. Thus

$$j_a^*(\epsilon^*) \simeq \frac{L_a^*}{4\pi V^*} \delta(\epsilon^* - 1). \quad (4)$$

Inserting this into equation (1) and integrating over ϵ , we find that the annihilation flux density integrated over photon energy has a beaming pattern $S_a \propto \mathcal{D}^4$.

Electron-positron thermal bremsstrahlung radiation will always accompany the annihilation radiation. At temperatures $\theta_a \gg 1$, the luminosity of e^+e^- bremsstrahlung can dominate e^+e^- annihilation radiation (see Skibo et al. 1995). For the temperatures we use in this paper, however, the bremsstrahlung flux is less than the fluxes of the other components, and is not included in the fits.

In addition to the annihilation radiation, we assume that there is an isotropic population of nonthermal pairs in the comoving frame with an energy spectrum given by a broken power law, so that

$$n_{\text{nth}}(\gamma, \mu, \phi) = \frac{k}{4\pi} \begin{cases} (\gamma/\gamma_b)^{-p_1} & \gamma_1 \leq \gamma \leq \gamma_b \\ (\gamma/\gamma_b)^{-p_2} & \gamma_b \leq \gamma \leq \gamma_2 \end{cases}, \quad (5)$$

where $p_2 = p_1 + 1$ and $p_1 \gtrsim 2$. Such a time-averaged particle spectrum might arise if shocks are present and radiative cooling is efficient for pairs in the high energy portion of the spectrum (Dermer & Schlickeiser 1993; Sikora, Begelman, & Rees 1994). We consider a situation where the particles scatter external ambient soft photons which are isotropic in the frame through which the radiating plasma moves (Sikora et al. 1994). If the photon energy is ϵ_0^* , then all scattering will take place in the Thomson regime if $\Gamma\gamma_2\epsilon_0^* \ll 1$. If the scattering takes place in the Thomson regime, then the approximation of Reynolds (1982) can be used to derive (see Dermer 1995; Dermer et al. 1997) the observed scattered flux density, given by

$$S_c(\epsilon; \mu, \phi) = \frac{L_C^* A \gamma_b^{p_i}}{d_L^2} \left(\frac{1 + \mu}{1 + \beta} \right)^{1 + \alpha_i} \mathcal{D}^{4 + 2\alpha_i} (1 + z)^{1 - \alpha_i} \left(\frac{\epsilon}{\epsilon_0^*} \right)^{-\alpha_i}, \quad (6)$$

for $i = 1, 2$, where $\alpha_i = (p_i - 1)/2$. When $i = 1$,

$$\gamma_1^2 \lesssim \frac{\epsilon(1+z)(1+\beta)}{\mathcal{D}^2 \epsilon_0^* (1+\mu)} \lesssim \gamma_b^2, \quad (7)$$

and when $i = 2$,

$$\gamma_b^2 \lesssim \frac{\epsilon(1+z)(1+\beta)}{\mathcal{D}^2 \epsilon_0^* (1+\mu)} \lesssim \gamma_2^2. \quad (8)$$

The term L_C^* in equation (6) represents the luminosity of Compton-scattered radiation measured in the comoving plasma frame. The factor A in the normalization of expression (6) depends only on kinematic quantities through the expression

$$A = \frac{3}{16\pi\Gamma^2\epsilon_0^*} \left[\frac{\gamma_b^{p_1}(\gamma_b^{2-2\alpha_1} - \gamma_1^{2-2\alpha_1})}{1 - \alpha_1} + \frac{\gamma_b^{p_2}(\gamma_2^{2-2\alpha_2} - \gamma_b^{2-2\alpha_2})}{1 - \alpha_2} \right]^{-1}. \quad (9)$$

The beaming pattern in equation (6) goes as $\mathcal{D}^{4+2\alpha}(1 + \mu)^{1+\alpha} \sim \mathcal{D}^{4+2\alpha}$ for scattered radiation. If $p_1 \simeq 2$, then the spectral index $\alpha \simeq 1/2$ at energies below the break energy, and $S_c(\epsilon) \propto \mathcal{D}^5(1 + \mu)^{3/2}$. Thus the scattered radiation is more highly beamed than the annihilation radiation, where $S_a \propto \mathcal{D}^4$. We note that if the emission is made by a radiation process which produces a photon source which is isotropic in the comoving frame, then $S(\epsilon) \propto \mathcal{D}^{3+\alpha}$. Such beaming patterns result from isotropically distributed electrons radiating synchrotron and synchrotron self-Compton emission in a spherical plasma blob (e.g., Marscher 1987). This gives a beaming pattern comparable to the annihilation radiation, and when such emission components dominate, we expect the ratios of the flux densities of synchrotron or synchrotron self-Compton and annihilation radiation to vary only weakly with observing angle.

The third spectral component we consider is the accretion disk radiation. If optically thin, this component is isotropic in the stationary frame and would only display an angular dependence if obscuring clouds or a dusty torus shadow the radiation. Such emission could arise from Comptonization of soft accretion disk photons by a hot disk corona (e.g., Haardt & Maraschi 1993). For simplicity, we model this component by an exponentially truncated power law. The observed flux density is then given by

$$S_d(\epsilon) = \frac{L_d(1+z)^{1-\alpha_d}}{4\pi d_L^2} \frac{\epsilon^{-\alpha_d} \exp[-(1+z)\epsilon/\Theta_d]}{\int_{\epsilon_c}^{\infty} d\epsilon \epsilon^{-\alpha_d} \exp(-\epsilon/\Theta_d)}, \quad (10)$$

where the disk luminosity is denoted by L_d .

In Fig. 1 we show spectra for various viewing angles, choosing $\Gamma = 5$. The pair temperature in the outflow is fixed at $\Theta_a = 0.5$ and the parameters of the nonthermal pair distribution are $\gamma_1 = 1$, $\gamma_b = 10^3$, $\gamma_2 = 10^6$, $p_1 = 2.1$ and $p_2 = 3.1$. We set $\alpha_d = 0.5$, $\Theta_d = 0.5$, and $\epsilon_c = 10^{-3}$ for the disk parameters and set the redshift $z = 1$. The disk luminosity L_d is assigned the value 10^{47} ergs s $^{-1}$. We set $L_C^* = L_d/\Gamma$. The reason for this choice is that the jet luminosity should normally be less than the disk luminosity, since the accretion power is supplying the jet luminosity, and the factor Γ^{-1} accounts for the additional power required by the bulk motion of the jet. For the annihilation luminosity, we take $L_a^* = 0.1L_C^*$.

As can be seen in Fig. 1, the disk radiation is independent of observing angle and the annihilation radiation is less beamed than the strongly anisotropic Compton-scattered radiation. For this simple model, the disk produces X-ray emission only, the Compton scattered radiation always dominates at gamma-ray energies above 10 MeV and the annihilation radiation appears as an enhancement in the MeV range which, for certain observing angles, can dominate the flux at MeV energies. Hence for small observing angles, the source appears as a gamma-ray emitting blazar with the luminosity dominated by high-energy gamma-rays and the source displays properties similar to a large fraction of the > 50 gamma-ray blazars detected with EGRET (see, e.g., von Montigny et al. 1995). At angles slightly off axis the high-energy radiation flux decreases and the bulk of the high-energy gamma-ray luminosity comes out in the MeV range. The annihilation feature can dominate at moderate observing angles. At larger angles, the disk radiation dominates the observed flux, although scattered jet radiation could make a substantial contribution to the flux at MeV energies (Skibo, Dermer, & Kinzer 1994). Note also that radio loud AGN could exhibit time-variable hardenings and features at MeV energies due to the electron-positron component, as suggested in the $\theta = 30^\circ$ panel in Fig. 1.

We use this model to fit the Comptel data for the blazars PKS 0208-512 at redshift $z = 1.003$ and PKS 0506-612 at $z = 1.093$ (Bloemen et al. 1995; Blom et al. 1995). In Figs. 2 and 3 we show the contemporaneous gamma-ray observations of these sources made with the Comptel and EGRET instruments on *CGRO*. The X-ray points are noncontemporaneous observations made with *ROSAT* (Brinkman et al. 1994). In these fits, we fix the relative luminosities of the various spectral components to satisfy $L_a^* = L_C^* = \Gamma^{-1}L_d$. For the case of PKS 0208-512, the bulk Lorentz factor $\Gamma = 3$, the inclination angle $\theta = 18^\circ$ and the luminosity $L_d = 10^{47}$ erg s $^{-1}$. For PKS 0506-612, we let $\Gamma = 11$, $\theta = 9^\circ$ and $L_d = 3 \times 10^{46}$ erg s $^{-1}$. All other parameters are the same as used for Fig. 1. The parameters used in the fits are not unique, but are typical for gamma-ray blazars. Thus if jets are composed of electrons and positrons which thermally annihilate, then the existence of a class of MeV blazars could be a straightforward consequence of the different beaming patterns of the radiations.

3. Discussion

In this paper, we have considered implications of the suggestion that the features in MeV blazars arise from thermal annihilation radiation in a relativistic jet, as suggested by previous authors (see Section 1). The existence of a class of MeV blazars can be understood by orientation effects if the beaming patterns of the nonthermal radiation is different from

that of the annihilation radiation. If the gamma rays are produced by nonthermal jet electrons scattering photons produced external to the jet, then the annihilation radiation has a broader beaming pattern. This could account for the existence of the class of MeV blazars, and would be consistent with unification scenarios for radio-emitting AGNs (see, e.g., Urry & Padovani 1995 for a recent review). Moreover, if this interpretation is correct, then we predict that radio galaxies will exhibit time variable hardenings and features at MeV energies which would correlate with increasing core dominance.

Gamma-ray observations of line features and contemporaneous VLBI measurements of transverse angular speeds from relativistic plasma outflows provide a method to determine the Hubble constant. The radio observations furnish the apparent speeds, and the gamma-ray observations give the Doppler and cosmologically shifted energy of the annihilation line. As noted earlier by Roland & Hermsen (1995), measurements of \mathcal{D} and the apparent superluminal speed can be used to determine the angle of the jet with respect to the observer and the bulk Lorentz factor Γ of the outflowing plasma. As shown in Appendix A, multiple contemporaneous observations of the shifted line energies and transverse angular speeds provide a method to determine the Hubble constant. This is an extension of the work of Schlickeiser & Dermer (1995), who proposed a model-dependent method for measuring \mathcal{D} from the broadband spectral energy distribution of blazars. If the MeV features can be conclusively identified with annihilation line signatures, then the procedure proposed here will provide a more definitive method for determining the Hubble constant from coordinated radio and gamma ray observations.

Arbitrary spectral lines emitted from the outflowing plasma jets can also be utilized by this method. The identification of spectral line features with a specific outflowing plasma blob is indicated at gamma-ray energies by time variability. Observations (Wehrle 1996) show that the emergence of a radio emitting feature in high-resolution VLBI maps is preceded by a gamma-ray flare. A better method would be through milliarcsecond imaging of spectral lines, which is presently only feasible at radio and optical wavelengths; high resolution optical imaging requires, however, bright sources of apparent magnitudes $m \lesssim 9$.

If it is established that the peaks of MeV blazars are a consequence of electron-positron plasma jets, then such a result would have important implications for processes which power jets in radio-loud AGNs, requiring energization of particles in the compact environment near the supermassive black hole. Additional measurements with Comptel on *CGRO*, and observations with more sensitive soft gamma-ray telescopes, such as the *INTEGRAL* telescope scheduled for launch early in the next millenium, could resolve the question of the composition of jets in AGNs and provide a test of this model.

The work of C.D. was partially supported by NASA DPR S-57770-F. R.S. acknowledges partial support by DARA (50 OR 9406 3). J.S. and C.D. acknowledge support from Office of Naval Research.

A. A Method for Determining the Hubble Constant

Here we show how gamma-ray observations may be used in conjunction with VLBI radio observations to measure the Hubble constant. Consider a source at redshift z which ejects two e^+e^- pair plasma blobs with velocities $\beta_1 c$ and $\beta_2 c$ at different times in the same direction θ measured with respect to the line of sight. Let δ_1 and δ_2 be the blueshifts of the annihilation line emitted by these blobs measured with γ -ray observations. We have

$$\delta_1 = [\Gamma_1(1 - \beta_1 \cos \theta)(1 + z)]^{-1}, \quad (\text{A1})$$

$$\delta_2 = [\Gamma_2(1 - \beta_2 \cos \theta)(1 + z)]^{-1}, \quad (\text{A2})$$

where $\Gamma_i = (1 - \beta_i^2)^{-\frac{1}{2}}$, $i = 1, 2$. Eqs. (A1) and (A2) assume that the peak of the annihilation radiation occurs at $m_e c^2$, whereas the peak of thermal annihilation radiation is blueshifted (Ramaty & Meszaros 1981). The blueshifting of the peak of the radiation can be accounted for by determining the temperature through the width of the emission feature. If this effect is properly taken into account, then δ_1 and δ_2 can be precisely determined.

Let μ_1 and μ_2 be the angular speeds of the two blobs determined from radio observations. The apparent speeds of the blobs in the plane of the sky are

$$\frac{d_M \mu_1}{c} = \frac{\beta_1 \sin \theta}{1 - \beta_1 \cos \theta} = (1 + z) \beta_1 \Gamma_1 \delta_1 \sin \theta, \quad (\text{A3})$$

$$\frac{d_M \mu_2}{c} = \frac{\beta_2 \sin \theta}{1 - \beta_2 \cos \theta} = (1 + z) \beta_2 \Gamma_2 \delta_2 \sin \theta. \quad (\text{A4})$$

where d_M is the proper motion distance. Setting the cosmological deceleration parameter $q_0 = 1/2$ the proper motion distance is a function of the cosmological redshift z and the Hubble constant H_0 (Weinberg 1972) through the expression

$$d_M = \frac{2c}{H_0} \left[1 - (1 + z)^{-\frac{1}{2}} \right]. \quad (\text{A5})$$

These five equations express the five unknown quantities d_M , θ , β_1 , β_2 and H_0 in terms of the measured quantities μ_1 , μ_2 , δ_1 , δ_2 and z . Solving equations (A1) and (A2) for $\cos \theta$ and equations (A3) and (A4) for $\sin \theta$, and equating the ratio $\tan \theta$ to eliminate θ , we obtain

$$\Gamma_2 = \frac{1}{\delta_2(1 + z)} + \left(\frac{\mu_2 \delta_1}{\mu_1 \delta_2} \right) \left[\Gamma_1 - \frac{1}{\delta_1(1 + z)} \right]. \quad (\text{A6})$$

Dividing equation (A3) by (A4) leads to

$$\Gamma_1^2 = 1 + \left(\frac{\mu_1 \delta_2}{\mu_2 \delta_1} \right)^2 (\Gamma_2^2 - 1). \quad (\text{A7})$$

Substituting (16) into (17) we arrive at the following expression for Γ_1 :

$$\Gamma_1 = \left[\frac{2}{\delta_1(1+z)} \left(1 - \frac{\mu_1}{\mu_2} \right) \right]^{-1} \left\{ 1 - \left(\frac{\mu_1 \delta_2}{\mu_2 \delta_1} \right)^2 + \left[\frac{\left(1 - \frac{\mu_1}{\mu_2} \right)}{\delta_1(1+z)} \right]^2 \right\}. \quad (\text{A8})$$

From equation (A1) we then determine θ , given by

$$\theta = \cos^{-1} \{ \beta_1^{-1} - [\beta_1 \Gamma_1 \delta_1 (1+z)]^{-1} \}. \quad (\text{A9})$$

Using equation (A3) for the proper motion, we obtain

$$d_M = \frac{c(\Gamma_1^2 - 1)^{1/2}}{\mu_1} (1+z) \delta_1 \sin \theta, \quad (\text{A10})$$

and finally from equation (A5) we find the Hubble constant, given by

$$H_0 = \frac{2c}{d_M} \left[1 - (1+z)^{-1/2} \right]. \quad (\text{A11})$$

REFERENCES

- Begelman, M. C., Blandford, R. D., & Rees, M. J. 1984, *Rev. Mod. Phys.*, 56, 255
- Blandford, R. D., & Levinson, A. 1995, *ApJ*, 441, 79
- Bloeman, H., et al. 1995, *A&A*, 293, L1
- Blom, J. J., et al. 1995, *A&A*, 298, L33
- Böttcher, M & Schlickeiser R. 1996, *A&A*, 306, 86
- Böttcher, M, Mause, H., & Schlickeiser R. 1997, *A&A*, in press
- Brinkmann, W., Siebert, J., & Boller, T. 1994, *A&A*, 281, 355
- Dermer, C. D. 1984, *ApJ*, 280, 328
- Dermer, C. D., & Schlickeiser, R. 1993, *ApJ*, 416, 484
- Dermer, C. D. 1995, *ApJ* 446, L63
- Dermer, C. D., Sturmer, S. J., & Schlickeiser, R. 1997, *ApJS*, in press
- Haardt, F., & Maraschi, L. 1993, *ApJ*, 413, 507
- Henri, G., Pelletier G., & Roland J. 1993, *ApJ* 404, L41
- Jauch, J., & Rohrlich F. 1976, *The Theory of Photons and Electrons* (New York: Springer-Verlag)
- Macomb, D. J. et al. 1995, *ApJ*, 449, L99
- Marcowith, A., Henri, G., & Pelletier, G. 1995, *MNRAS*, 277, 681
- Marscher, A. P. in *Superluminal Radio Sources*, ed. J. A. Zensus & T. J. Pearson (New York: Cambridge University Press), p. 280
- Marscher, A. P., & Travis, J. P. 1996, in *Proceedings of the Third Compton Symposium*, Munich, Germany, 12-14 June, 1995, to be published in *A&AS*, in press
- Ramaty, R. & Meszaros, P. 1981, *ApJ*, 250, 384
- Roland, J., & Hermsen, W. 1995, *A&A*, 297, L9
- Schlickeiser, R., & Dermer, C. D. 1995, *A&A*, 300, L29; (e) 1996, 306, 675
- Schubnell, M. S., et al. 1996, *ApJ*, 460, 644
- Sikora, M., Begelman, M. C., & Rees, M. J. 1994, *ApJ*, 421, 153
- Skibo, J. G., Dermer, C. D., & Kinzer, R. L. 1994, *ApJ*, 426, L23
- Skibo, J. G., Dermer, C. D., Ramaty, R., & McKinley, J. M. 1995, *ApJ*, 446, 86; (e) 1996, 463, 391

Svensson, R. 1983, ApJ, 270, 300

Thompson, D. J., et al. 1995, ApJS, 101, 259

von Montigny, C., et al. 1995, ApJ, 440, 525

Weinberg, S. 1972, Gravitation and Cosmology: Principles and Applications of the General
Theory of Relativity (New York: John Wiley & Sons)

Williams, O. R., et al. 1995, A&A, 297, L21

This preprint was prepared with the AAS L^AT_EX macros v4.0.

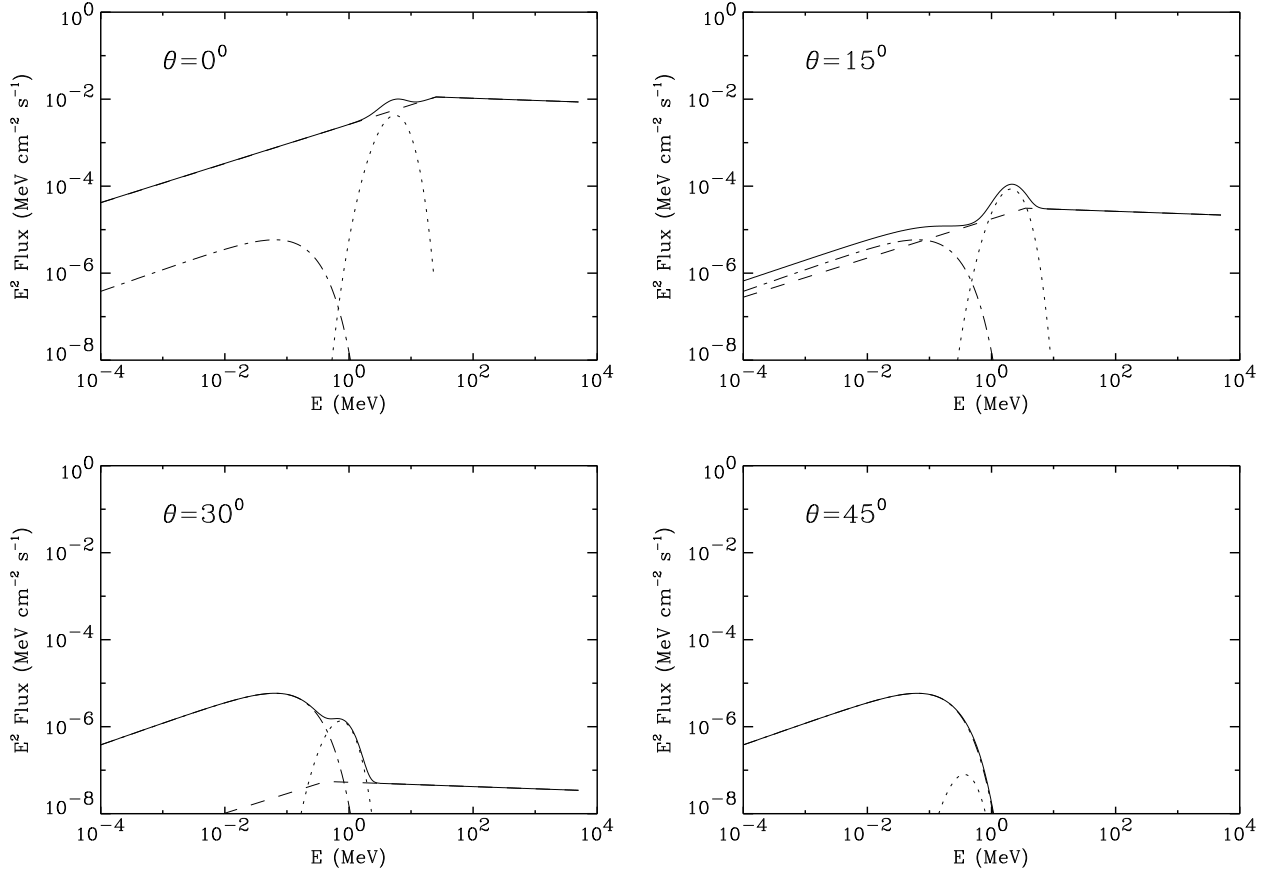


Fig. 1.— Spectra for various viewing angles and bulk Lorentz factor $\Gamma = 5$. The dashed curves represent the observed flux produced by inverse Compton scattering of isotropic soft photons by nonthermal pairs in the relativistic outflowing plasma jet, the dotted curves are the observed fluxes of thermal pair annihilation radiation produced in the jet, and the dot-dashed curves are the optically thin isotropic emission produced by an accretion disk corona. The solid curves give the total fluxes. See text for parameter values.

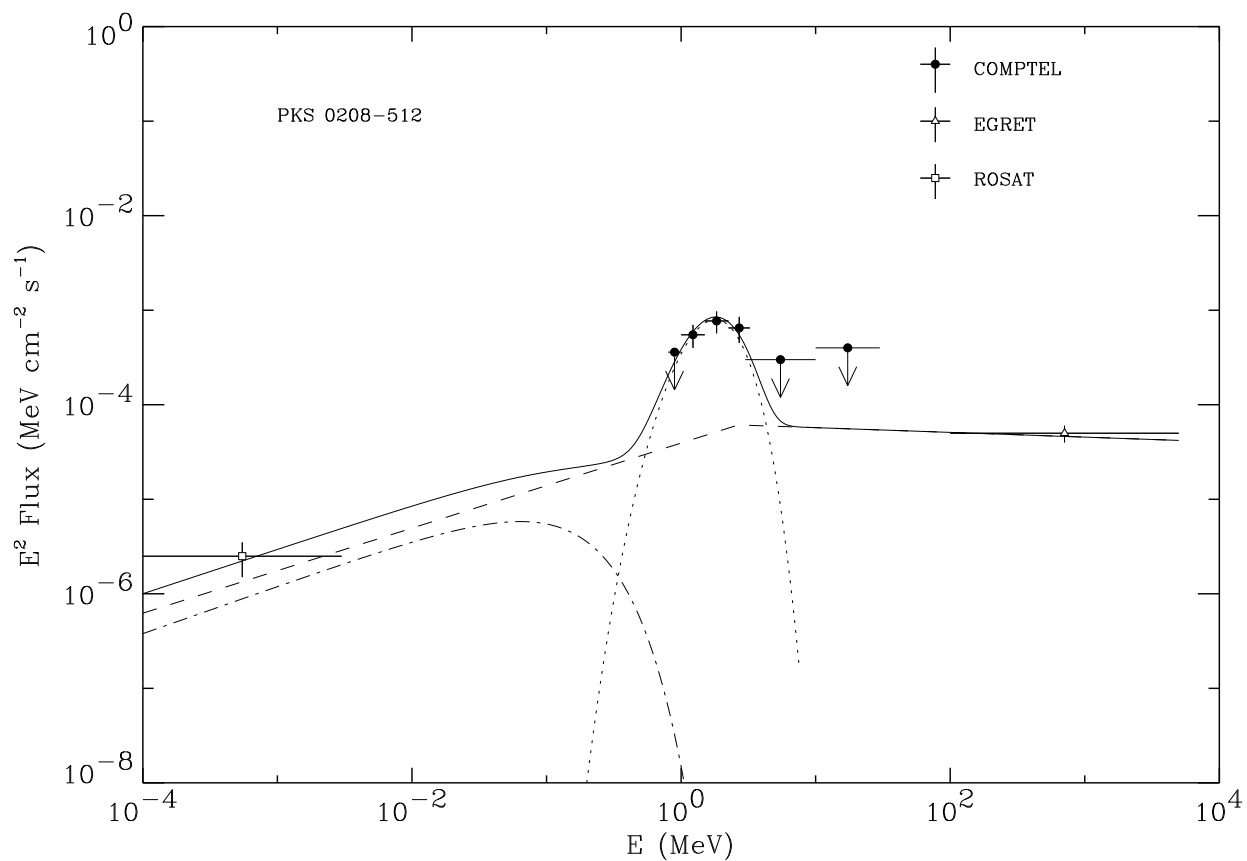


Fig. 2.— *High-energy spectrum of PKS 0208-512. The individual components are specified by the curve types as in Fig. 1. The parameters are $\alpha_d = 0.5$, $\Theta_a = \Theta_d = 0.5$, $\epsilon_c = 10^{-3}$, $\gamma_1 = 1$, $\gamma_2 = 10^6$, $\gamma_b = 10^3$, $p_1 = 2.1$, $p_2 = 3.1$, $\Gamma = 3$ and $\theta = 18^\circ$.*

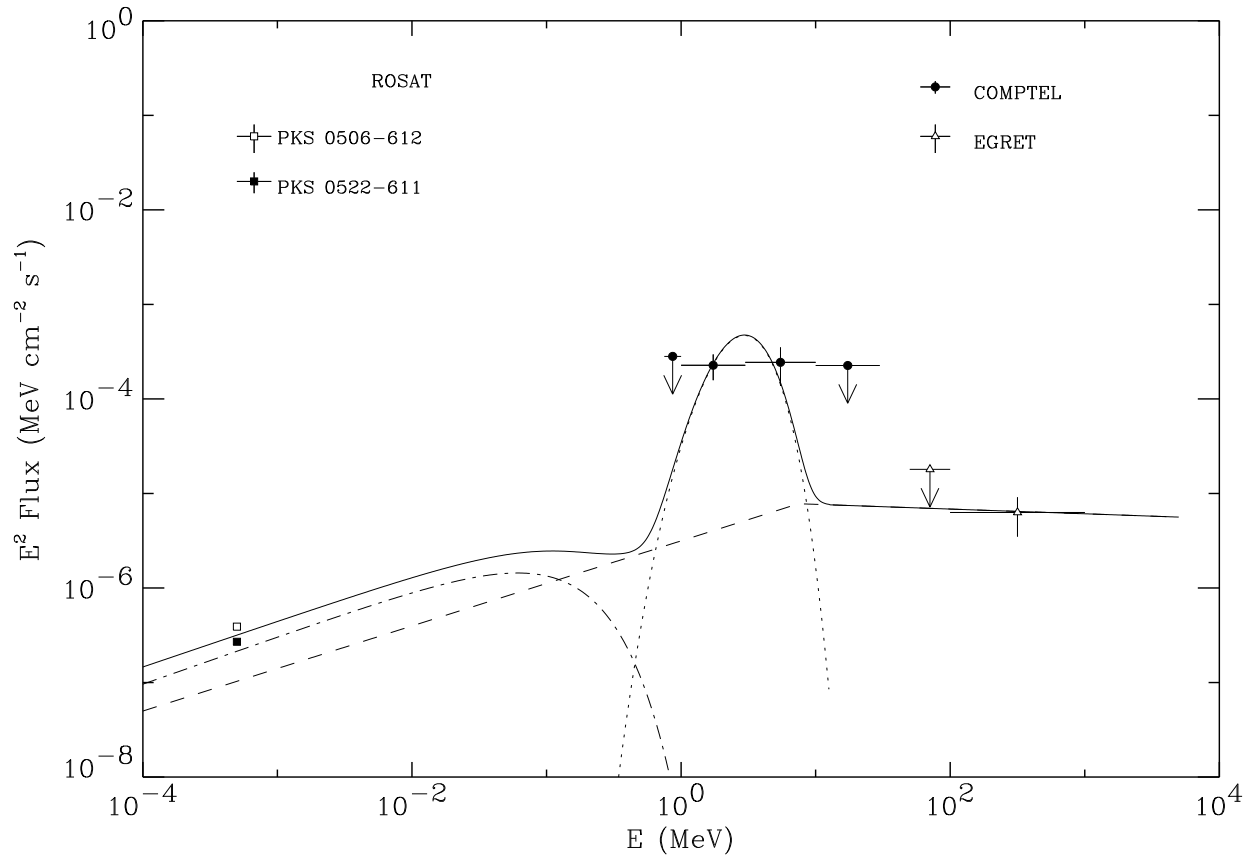


Fig. 3.— *High-energy spectrum of PKS 0506-612. The individual components are specified by the curve types as in Fig. 1. The parameters are the same as in Figure 2 except $\Gamma = 11$ and $\theta = 9^\circ$.*